# Addressing the correlation between binocular rivalry and visual temporal resolution: An indirect test of Alpha oscillations in visual perception

Master thesis in Brain and Cognition

Author: Carla Morante Alberti

Supervisor: Mireia Torralba Cuello

Co-supervisor: Salvador Soto Faraco

5 of July 2021

Universitat
Pompeu Fabra
Barcelona

## Table of contents

## Abstract

Alpha oscillations are thought to act as an internal brain pacemaker that serve to modulate the perception of visual information in a phasic manner. The so-called perceptual cycles hypothesis suggests that alpha cycles consist of windows of perceptual integration -whose frequency modulates what is perceived sequential or simultaneous. The present study addresses this hypothesis with an indirect test of alpha oscillations in visual perception. We measured Binocular Rivalry (BR) dynamics together with the two-flash fusion to test a potential positive correlation of the speed of perceptual alternations in BR and the visual temporal resolution in human adults (11 female, 9 male). The results showed a moderate evidence in favour of null correlation ($BF_{0-} = 6.634$). A post-hoc two-sided test revealed anecdotal evidence in favour of no correlation between these variables. Despite the findings did not support the prediction that faster alternations in the BR task correlate with lower thresholds in the two-flash fusion task, they do not necessarily imply a contradiction of the hypothesis of alpha oscillations as a visual information sampling mechanism. Tentative explanations based on task-dependent individual alpha frequency modulation allow the results to fit in the perceptual cycles hypothesis framework although additional EEG measurements would be needed to corroborate it.

## 1. Introduction

The aim of this empirical study is to address the potential correlation between bistable perception in Binocular Rivalry and temporal resolution in vision.

The introduction, hypothesis, methods, sample size estimation and analysis pipeline were pre-registered in the Open Science Foundation web before any analyses were performed (https://osf.io/ju4cg/). At the pre-register moment, we had collected data from 14 participants.

### 1.1 Bistable perception

Visual perception depends not only on incoming retinal input, but also on cognitive processes and endogenous brain activity. Current views consider vision as an active inferential process rather than mere passive processing of sensory input (Pylyshyn, 1999; Von Stein, Chiang and König, 2000; Engel, Fries, and Singer, 2001; Gilbert and Sigman, 2007). At a physiological level, these inferential processes rely on recurrent networks involving top-down processing. Such top-down contributions to vision are the responsible for the well-known phenomenon of bistable perception: having multiple perceptual interpretations of the same sensory input despite it remains physically constant (e.g., Leopold and Logothetis, 1999). When this situation occurs, subjective perception alternates between the different possible interpretations in a stochastic manner, as in the particular case of ambiguous images containing two possible interpretations, such as the Necker Cube (Necker, 1832) or even some famous artistic paintings (Fig. 1).

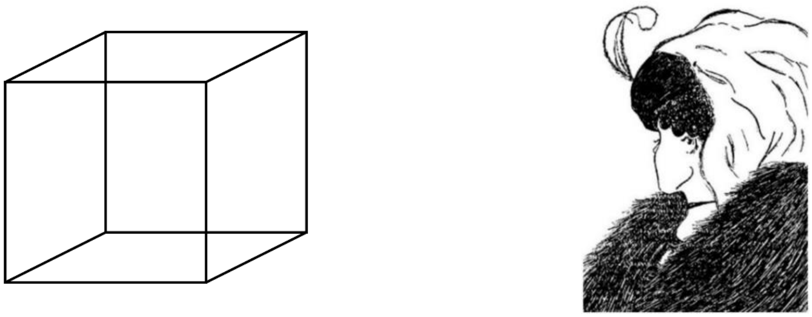

**Figure 1.** Left: Necker Cube. Right: Picture of “My Wife and My-Mother-in-Law” by American cartoonist William Ely Hill.

The phenomenon of bistable perception has been widely used in the study of consciousness for many decades since it provides a well-controlled experimental approach to study the brain's processing when it is faced with ambiguities in sensory inputs (Crick and Koch, 1998; Rees et al., 2002; Blake, Brascamp, and Heeger, 2014). Indeed, depending on the stimulus, we can differentiate between two types of bistable perception: when a stimulus does not contain enough information to form one unique percept, as the Necker Cube, or when it provides conflicting information that can be interpreted in two different ways, like Binocular rivalry (Mamassian and Goutcher, 2005).

### 1.2 Binocular Rivalry

One paradigmatic case of bistability is binocular rivalry (Blake, 2001; Tong, 2001; Blake and Logothetis, 2002; Alais and Blake, 2005). Binocular rivalry occurs when each of the observer's eye views incompatible images at the same retinal location simultaneously, referring to "incompatible" as sufficiently different stimuli to prevent binocular fusion (a process whereby we normally extract depth information during natural vision; Blake and Wilson, 2011). Perceptually, binocular rivalry is experienced as random fluctuations between one image and the other (Tong, Meng and Blake, 2006), spending almost the same amount on each one if they are equally salient (Fig. 2).

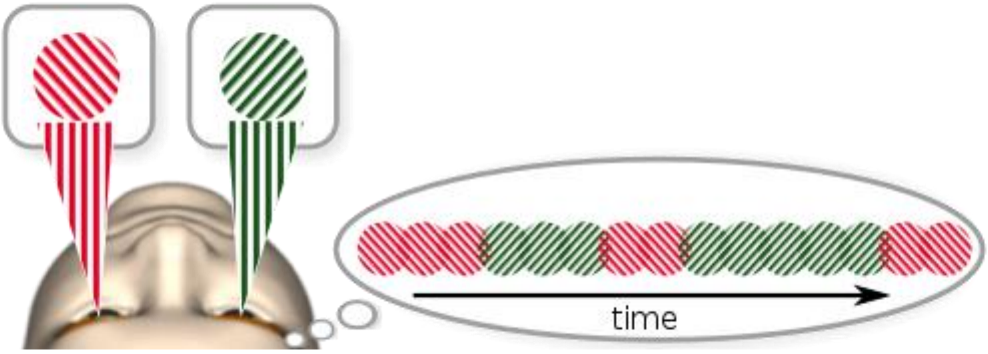

**Figure 2.** Schema of the BR phenomenon. Left: Rival stimuli presented to each eye. Right: Perception across time. Extracted from Hedger (2019).

Although stimulus saliency, governed by low-level features such as orientation, contrast and colour (Blake, 2001) has a large role stimuli alternation, top-down processes as endogenous selective attention have been shown to impact on binocular rivalry dynamics as well (Paffen and Alais, 2011; Zhang et al., 2011). Despite the neural basis of this phenomenon remains still unclear, many theories point out at a competition occurring between two pools of neurons, each representing one of the rival stimuli (Alais and Blake, 2005; Freeman, 2005). This competition may arise from monocular neurons in early stages of the visual pathway, that is V1 (Tong et al. 1998; Polonski et al. 2000) or at higher stages of visual processing, such as a competition between incompatible pattern representations (Leopold and Logothetis, 1996; Tong et al., 2006). The competition, as well as the continuous re-evaluation process producing the fluctuations in the outcome is what is thought to result in the bistable perception phenomenology.

The mean frequency of alternation between rival percepts in BR is defined as the Natural Alternation Rate (NAR). Interestingly, NAR is relatively characteristic for each subject, but there exists large interindividual variability (Kleinschmidt et al., 2012). The stability of NAR within individuals has led to the suggestion that it depends on genetically hereditary factors as it has been tested with monozygotic twins (Miller et al, 2010). Indeed, the intra-individual reproducibility of NAR is not restricted to BR, but several correlations across different forms of bistable perception and stimuli within individuals have been reported (Carter and Pettigrew, 2003; Brascamp, Van Ee et al. 2005). The stability across tasks and time, make the NAR a potentially important cognitive biomarker. Albeit the NAR depends on properties of the rival stimuli, such as their saliency (Kang, 2009), or of the individuals, such as their age (Ukai et al., 2003), these variables can be controlled leading to the question of why there exists such an inter-subject variability in the alternation rate. More specifically, which is the mechanism underlying this characteristic and stable alternation rate?

### 1.3 Brain oscillations: Alpha activity

Several studies link BR with oscillatory activity in the brain (Piantoni et al., 2010, Cha and Blake, 2019), which is representative of cyclic changes in the excitability of neural populations. Particularly, it has been linked to the alpha band (8-13 Hz), (Pápai et al., 2018, Katyal, 2019, Luo and Van Rullen, 2021).

Occipital alpha activity, first discovered by Berger (1929), is the most prominent rhythm in the human brain. Since the initial observations, alpha oscillations have been specially related with attention (Foxe and Snyder, 2011; Thut et al., 2006; Haegens et al., 2012) as well as other cognitive functions such as memory

(Klimesch, 1999, 2012). Numerous studies attribute an inhibitory role to alpha oscillations, linking high alpha power to high inhibition. That is, during a task, alpha power typically increases in task irrelevant brain areas in order to inhibit processing, whereas it decreases in task relevant areas, releasing them from inhibition. This gating by inhibition hypothesis (Jensen and Mazaheri, 2010; Klimesch et al., 2007) suggests that alpha activity serves to functionally disengage a given region by means of "pulsed inhibition", considering not only its amplitude but also a phasic mechanism. In line with this hypothesis and considering the idea of a mechanism that samples the visual input into discrete windows of optimal perception, Varela et al. (1981) first proposed occipital alpha oscillations to be this sampling mechanism for visual perception. Recently, Van Rullen (2003) brought back the old question of whether visual perception is discrete or continuous encouraging further investigation that serves to support the alpha oscillations' role in the perceptual cycles hypothesis.

### 1.4 Perceptual cycles

The perceptual cycles hypothesis (e.g., Van Rullen, 2016) suggests that occipital alpha oscillations provide phases of optimal perception and phases of inefficient perception, which is supported by previous psychophysiological and electrophysiological experiments (Busch et al., 2009; Dugué et al., 2011, Haegens et al., 2011; Chakravarthi & VanRullen, 2012; Samaha and Postle, 2015; Harris et al., 2018). Evidence from these studies pointed toward a modulation of visual perception through both occipital alpha amplitude and phase, resulting in a rhythmic or even discrete perception, in the most extreme interpretation of their hypothesis. In the soft version of the hypothesis (i.e. rhythmic perception), for each cycle of alpha oscillation, there is a particular phase that gives rise to more efficient perceptual processing, whereas the same process is less efficient at the opposite phase (Fig. 3A). In their extreme version, alpha oscillation phase serves to separate perceptual events into discrete epochs, like snapshots of the visual input (Fig. 3B), modulating thus, the temporal parsing of perceptual events.

Perceptual cycles can be considered as windows of temporal integration in which all the input visual information occurring within this window is perceived as simultaneous. Instead, sensory inputs occurring at different windows, would be perceptually separate. Thus, this idea explains why two visual stimuli in a sequence are sometimes perceived as simultaneous (single unique percept), while sometimes are perceived sequentially (individual events) (Fig. 3C). This idea implies that perception depends not only on the oscillation phase, but also on its frequency (Fig. 3D,E). That is, the two visual stimuli are integrated in the same temporal window (simultaneous) or there is a sampling between them (sequential).

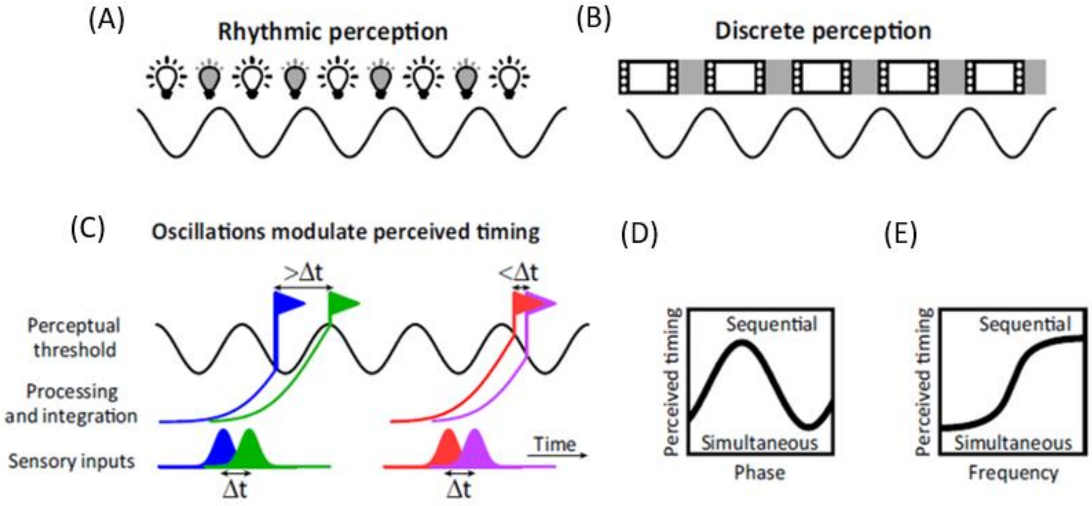

**Figure 3.** Perceptual cycles. (A) Soft version of the perceptual cycles hypothesis represented as optimal phases for perception (bright light bulbs) and not efficient phases for perception (dimmed light bulbs). (B) Extreme version of the perceptual cycles hypothesis represented as discrete events framed by the occipital alpha oscillations. (C) Perceived timing for the same sensory inputs depending on the ongoing oscillations. Blue and green stimuli perceived as sequential whereas red and purple stimuli perceived a simultaneous. (D,E) Prediction of the perceived timing depending on the alpha oscillations phase and frequency. Adapted from Van Rullen (2016).

However, there are other evidence that do not support the perceptual cycles hypothesis since they have found that only the power, but not the phase, of neural oscillations occurring immediately before the visual stimulus presentation can predict the stimulus perception (Benwell, 2017; Ruzzoli, Torralba et al., 2019). Indeed, recent studies point towards the prediction of conscious awareness but not visual sensitivity with prestimulus alpha-band power (Samaha, Postle et al., 2017, 2020; Benwell et al., 2021).

## 1.5 Individual Alpha Frequency (IAF)

The findings and theory described above propose phasic modulation of perception. Consequently, if this hypothesis is true, the frequency of alpha oscillations has a key role in visual perception modulation. In support of this idea, several studies found correlations between individual alpha frequency (IAF) and various aspects of visual processing (Samaha and Postle, 2015; Cecere and Romei, 2015, Migliorati et al., 2020), which have been lately replicated using rhythmic entrainment via periodic visual stimuli or alpha-TMS (Minami & Amano, 2017; Chota and Van Rullen, 2019; Gulbinaite et al., 2017).

The individual alpha frequency can be estimated as the frequency corresponding to the local maximum in the individual's EEG power spectral density, within the alpha range (Fig. 4). The IAF is characteristic for each person, meaning that it presents a high inter-subject variability and, as well as the NAR, it is heritable and stable within healthy individuals. It reflects systemic properties of the brain and relates to cognitive functioning (Grandy et al., 2013). Despite alpha oscillations are usually defined within the interval 8-13 Hz, individual measures can be found below and over this range (Aurelien et al., 2004).

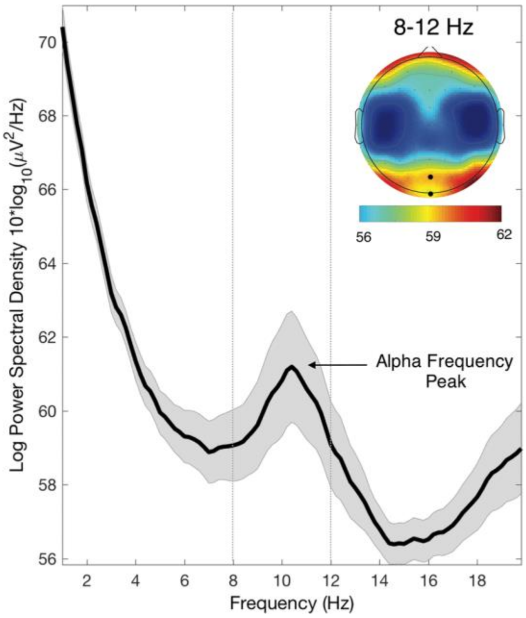

**Figure 4.** Individual alpha frequency IAF peak detection. Plot of the power spectral density (PSD) of a resting-state EEG in the electrodes Oz and POz. Topographical map at the top depicts PSD (dB) for the alpha frequency band. Extracted from Ronconi and Busch, 2018.

Although the vast majority of IAF correlations are shown with the temporal resolution in visual tasks (Samaha and Postle, 2015; Milton, 2016; Ronconi, Busch, Melcher, 2018; Chota and Van Rullen, 2019, Wutz, 2018), there are reports of other correlations such as with the amplitude of visual evoked potentials and hemodynamic responses (Koch et al., 2008), the speed of processing information (Klimesch et al., 1996), and the perception of illusions (Cecere and Romei, 2015). However, studies that support the perceptual cycles hypothesis with causal contributions of neural oscillations at the alpha frequency can be split in two different categories: temporal resolution (Ronconi, Busch, Melcher, 2018; Chota and Van Rullen, 2019) and BR (Kaytal et al. 2019; Torralba et al., 2020).

### 1.6 IAF in BR

Katyal et al. (2019) and Torralba et al. (2020) have recently found a positive correlation between IAF and NAR in a BR task. Torralba et al. (2020) demonstrated a causal frequency-specific modulation of BR dynamics using visual entrainment. However, there is a ten factor difference between the temporal scale of the two phenomena since perceptual fluctuation in BR usually happens at around 1 Hz, while alpha oscillations happen at around 10 Hz. Torralba et al. (2020) suggested that the function of Alpha cycles is to open a re-evaluation window in the competition between the two stimuli (rival images) without interfering with the two signals, but just accessing to the outcome of the competition between the neuronal representations. Thus, faster oscillations (faster IAF) imply more evaluation windows per unit of time, resulting in higher probability to see a change in the competition outcome that is reflected in a perception change or alternation. Meaning that, individuals with higher IAF tend to perceive more alternations.

### 1.7 IAF in temporal resolution

If alpha oscillations sample visual input into discrete windows of temporal integration, then intuitively the perceived timing of events will be modulated by this sampling frequency that corresponds on average to the IAF. Samaha and Postle (2015) first showed that the individual speed of alpha oscillations was predictive of the temporal resolution of visual perception, using a two-flash fusion task. Individuals with higher alpha frequencies showed finer visual temporal resolution. This finding is not restricted to visual temporal resolution since this same behaviour was reflected in the double flash illusion which involves cross-modal integration (Cecere and Romei, 2015, Migliorati, 2020). Recently, several studies provided evidence for a direct and causal link between changes in the alpha frequency and the temporal resolution of perception using, for instance, audio-visual entrainment (Ronconi, Busch, Melcher, 2018), visual entrainment at the alpha frequency (Minami and Amano, 2017; Chota and Van Rullen, 2019) or even brain stimulation such as TMS (Chota and Van Rullen, 2020) or transcranial alternating current stimulation (Battaglini et al., 2020).

### 1.8 Summary and scope of the present study

Briefly summarizing, it has been shown with correlations as well as with causation protocols that individual alpha frequency modulates individual alternation rate in a BR task and in visual temporal resolution tasks, using different protocols and in different studies. Both give physiological as well as behavioural evidence in the direction of the perceptual cycles hypothesis, since they propose alpha oscillations to cyclically provide windows of evidence accumulation: in one case for the re-evaluation of rival stimuli representation and, in the other, for the visual input integration.

We want to put the last piece of this puzzle addressing the potential correlation between the speed of perceptual alternations in a BR task (NAR) and visual temporal resolution in a two-flash fusion task. The aim is to provide a more complete picture of the potential role of alpha in the perceptual cycles theory in an indirect way. There is a large literature that supports the link of alpha frequency with visual temporal resolution, but only few recent papers relating it to the alternation rate in the BR task. Therefore, this study also will serve to make the evidence for the latter finding more robust or to question it.

## 2. Hypothesis of the current study

Based on the previous literature, we hypothesize that if alpha is related, on one side, to visual temporal resolution and, on the other, to the speed of perceptual alternations in BR, there should exist a correlation between the NAR and visual temporal resolution. According to this hypothesis, we predict that higher temporal resolution in a two-flash fusion task will correlate positively with the natural alternation rate in a BR task.

## 3. Materials and Methods

Given the aim to evaluate the correlation between the NAR in a BR task and the visual temporal resolution in a two-flash fusion task, every subject has performed these two tasks in the experiment. The task order has been randomized across participants: half of the participants first completed the BR task and then performed the two-flash fusion task, whereas the other half of participants first completed the two-flash fusion task and then they performed the BR task. Both tasks were performed on the same session, and the total duration of the experiment was approximately 70 min, including a 5 min break between tasks.

In both tasks, stimuli were presented on a 32’’ Display ++ monitor (100 Hz refresh rate) placed at 80 cm from the subjects’ head. Visual stimuli for the two experiments was created and presented using the Matlab toolbox Psychtoolbox (Psychophysics Toolbox, RRID:SCR_002881), version 3.

### 3.1 Binocular Rivalry task

Stimuli consisted of two circle-shaped Gabor patches (Michelson contrast 0.1) in colours red and green, orthogonally oriented (±45º off vertical), surrounded by a black circular ring. The background of the screen was grey. Both patches, 11.5º in diameter, contained a central fixation cross identical in each of the patches (Fig. 5A).

The red luminance was fixed for all participants at 255 RGB. In order to avoid dominance of one of the stimuli (red or green), the green luminance was manually adjusted by each participant until he/she subjectively matched the luminance with the red stimulus. To do that, we first presented participants with central alternating green and red stimuli (at 60 Hz rate). Subjects were asked to adjust the luminance of the green stimulus until the flickering was minimized (Cavanagh et al., 1987).

During BR task, participants were presented with one stimulus to each eye by means of stereoscopic mirror goggles, as in Figure 5B, which prevents each eye to see the contralateral stimulus.  This required a first calibration of the mirrors in which participants were asked to match the positions of two separated stimuli presented on the left and right hemifield, respectively, by adjusting the mirrors’ orientation using a wheel in each side of the goggles. The calibration was performed after the isoluminance adjustment.

Participants' task consisted on reporting the instantaneous percepts by key pressings in a standard keyboard. That is, they had a specific key ('X' or 'D') to report when they saw the green stimulus and the other one to report that they were perceiving the red stimulus ('D' or 'X', respectively). The intermixed percept, defined as a mixture of the two percepts, was reported by pressing both keys ('X' and 'D'). No percept (i.e. grey background) was reported by releasing both keys (No key press) (Fig. 5C). We randomized the key mapping across participants: half of the participants used the 'X' key for red percept and 'D' key for green percept and the contrary mapping for the other half of participants. The position of the stimuli presentation was also randomised, that is, half of the blocks the red stimulus appeared on the left of the screen and the green on the right, whereas the other half of blocks, the green stimulus appeared on the left and the red on the right of the screen.

The protocol consisted of 8 blocks of 120 seconds length, separated by self-paced resting intervals. Before the testing task started, the participants performed a single training block of 2 minutes in which we made sure that the subject understood the task correctly.  The number of blocks has been chosen in order to ensure enough number of percepts for a stable estimation of the NAR based on previous experiments using these stimuli (https://osf.io/w8m4q/), and have a reasonable duration of the experiment, to avoid subject's fatigue (see sample size estimation).

The total task time was approximately 30 minutes, including the isoluminance adjustment, the goggles calibration, the training and the test trials.

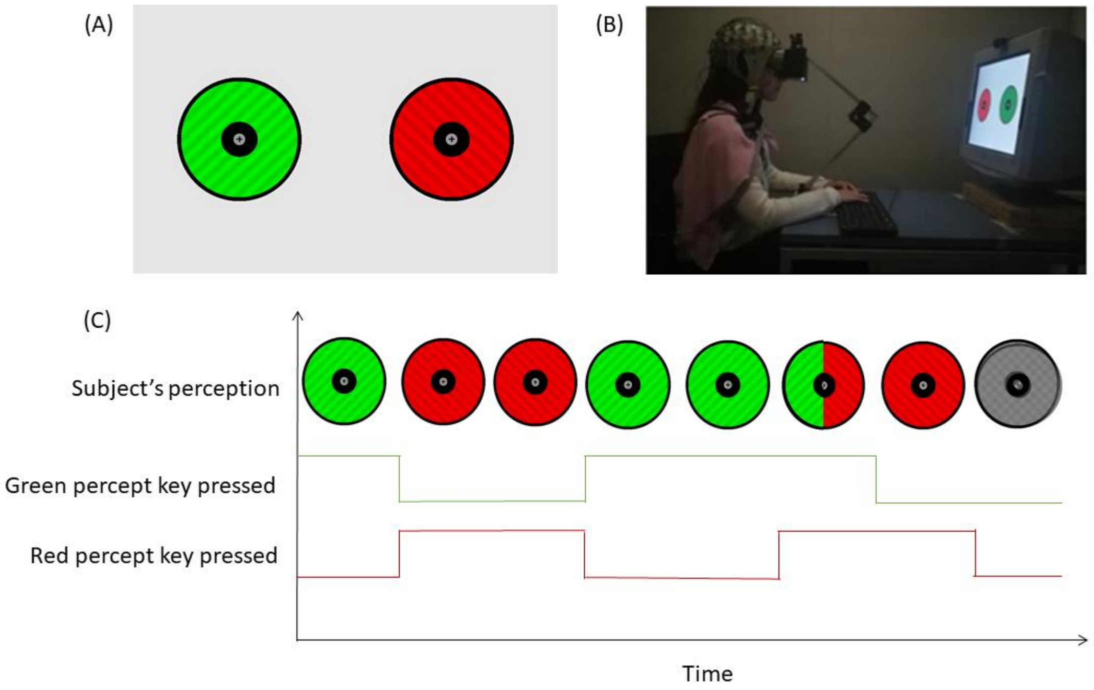

**Figure 5.** Binocular Rivalry experiment. (A) Stimuli presented in the experimental paradigm. (B) Image of the experimental setup with the stereoscopic mirror glasses. (C) Example of a subject's perception reporting by means of the key pressings. When the line is up means the corresponding key pressed whereas when the line is down, it means the corresponding key is not pressed.

### 3.2 Two-flash fusion task

The two-flash fusion task used the same behavioural paradigm as Samaha and Postle (2015). The trial started with a white fixation cross in the center of the screen that prepared subjects for the incoming stimuli by dimming (Fig. 6A). The duration of this warning period was a random time between 400 and 800 ms. Then, the flash event was presented. On half of the trials, the flash event was composed by two flashes that were presented either both to the left or both to the right of the dimmed fixation cross with equal probability. On the other half of the trials, the flash event consisted of one single flash presented either to the left or to the right of the dimmed fixation cross with equal probability. (The timings of these flash events are specified below). After the flash event, a blank screen with only a dimmed fixation cross was presented during 800 ms, followed by the response period indicated by the brightening of the fixation cross. Participants' task was to report whether they had seen one flash or two flashes in the response period on a right-handed button press on a computer keyboard, using their index finger to press the “1” key and their middle finger to press the “2” key, to indicate one or two flashes, respectively. The next trial did not begin until the participant had responded. Participants were asked to stress accuracy over speed of their responses.

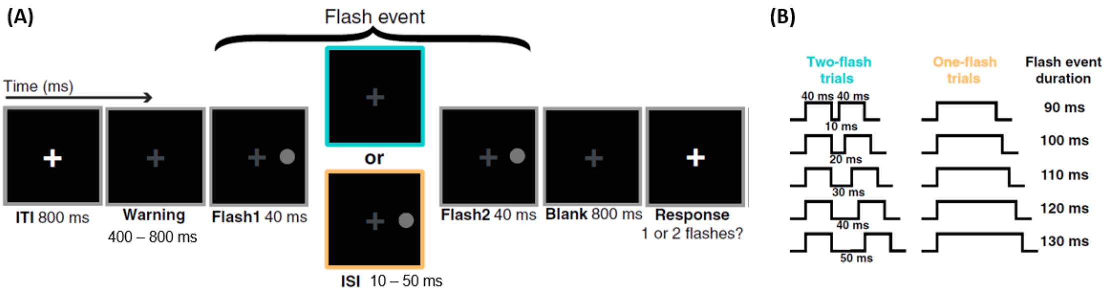

**Figure 6.** Two-flash fusion paradigm. (A) Trial (B) Timing of the stimuli presentation in the two conditions: two flashes versus one flash. The total amount of time of the two different flash events for each ISI is the same.  From Samaha and Postle (2015).

The flash stimulus consisted of a grey disk (diameter: 1.23 degrees of visual angle; luminance: 0.62 cd/m$^2$) that was presented left or right of the fixation cross at 2.45 degrees of visual angle. In the two-flash trials, the stimuli consisted of two disks presented during 40 ms, separated by the interstimulus interval (ISI), which consisted on a blank screen with a dimmed fixation cross. The ISI varied from 10 to 50 ms in 10-ms steps, i.e., 10, 20, 30, 40 or 50 ms. On the one-flash trials, one single disk stimulus was presented with a duration that varied to match the first disk onset to the second disk offset of the two-flash trials, at each ISI, so that the total stimulus duration did not inform the participant of the number of flashes (Fig. 6B). Stimulus timing was verified with a photodiode, using the Black Box ToolKit v2, to a resolution of 1 ms.

For training, prior to the actual task, participants were presented with 20 trials in which we showed them 10 examples of one-flash trials and 10 examples of two-flash trials, with two trials per ISI ordered from less to more difficulty. After the example trials, subjects completed 30 training trials with trial type, ISI and stimulus location randomized, just like in the actual task blocks. Then, participants completed 500 test trials divided into 5 blocks of 100 trials with self-paced breaks in between each block. Within each block, we randomly presented 10 repetitions of each ISI per trial type. Participants were informed of the equal probability that one or two flashes appeared. The two-flash fusion task lasted for approximately 40 minutes, including the example trials, the training and the test trials.

## 4. Trial number and sample size estimation

### 4.1 Number of blocks for the BR experiment

We used the results from Torralba et al., 2020 in which they shown that with 5 blocks of 120 seconds, they could already achieve a stable estimation of the NAR. Particularly, with 8 blocks the deviation of the NAR from a reference value obtained with 9 blocks was about 2% (see Appendix A).

### 4.2 Number of blocks for the two-flash fusion task

Based on Samaha and Postle (2015), we reduced the number of trials from 600 to 500, without modifying the number of trials per block. Thus, we had 5 blocks instead of 6. The decision was based on the fact that subjects were performing two tasks in the same session, in order to keep the duration of the experiment reasonably long, to avoid subject's fatigue.

Due to an error, two of the subjects had 450 trials in the two-flash task, instead of 500 (250 two flash trials, 200 one flash trials). These two subjects were included in the analysis.

### 4.3 Sample size

Due to the lack of previous similar experiments, we could not make an informed estimation about the effect size. We decided to run a minimum of 20 subjects and set a stopping criterion based on a Bayesian approach (see Statistical analyses), with a maximum of 50 subjects, based on experiment cost and time.

## 5. Analysis

In the BR experiment, we measured the Natural Alternation Rate (NAR), that is the inverse of the natural alternation time (NAT). The NAT is the median time between reporting two different pure percepts (Davidson et al., 2018), that means, Red to Green or Green to Red. Therefore, to compute the NAR we only considered the time length of the pure percepts, discarding periods of intermixed percept and no clear percept. Data from Red and Green percept was pooled together as we had no interest in dominance differences. We filtered out from the analysis percepts shorter than 300 ms (estimated latency of the motor evoked potential from key presses (Halgren, 1990)) and percepts longer than 100 s since the block lasted for 120s -meaning that the subject was not experimenting alternation within the block.

For the two-flash fusion experiment, we fitted a psychometric function for each subject using the Quickpsy package (Linares and López-Moliner, 2016) in an R environment (Team, 2013). The proportion of correct response at each ISI, regardless the type of trial (i. e. one-flash and two-flash trials) and the right or left appearance in the screen, was fitted with a logistic function with four parameters: the threshold, the slope, the guess rate and the lapse rate. Data from left and right stimuli were pooled together as we did not expect different temporal resolutions at the right and left hemifield. The guess rate was fixed at 0.5, that is at chance level since it is a 2AFC task. The threshold and the slope were free to estimate parameters. The lapse rate -probability of an incorrect response regardless of the stimulus variable parameter- was set as a free to estimate parameter in the pre-register, following Wichmann and Hill (2001). However, once we looked at the data, we realised that we had no sufficient points in the superior asymptote of the psychometric curve to make a good estimation of the lapse rate, therefore, we found that some curves did not converge. As some studies suggest, it is a better fitting model to fixate the lapse at 0 than to estimate it when there is no sufficient data in the saturation interval (Prins, 2012; Linares and López-Moliner, 2016), so finally we had fixated the lapse rate at 0, obtaining a convergence for all the subjects as we can see in Appendix C.

To estimate the goodness of fit, we computed deviance of the fit from the original dataset (Wichmann and Hill, 2001). The deviance is defined as the log-likelihood ratio between saturated and best fit and it gives an idea of how much the saturated model -that is, a model with no residual errors between the actual data and model predictions- deviates from the best fit found for the data and its p-value. To calculate the p-value, we generated 1000 bootstrap samples that were fitted and computed its deviance, obtaining a deviances distribution. Given the distribution, p-value is calculated as the probability of obtaining a larger value of the deviance than the deviance calculated for the original data. Once the psychometric function was fitted, we measured the two-flash fusion threshold for each subject, defined as the approximate ISI at which the predicted discrimination accuracy was 75%.

### 5.1 Statistical analyses

We decided to perform sequential testing in order to decide the final sample size (Schönbrodt, 2017). To avoid an increase in type I errors, we used one tailed Bayes factor (Wagenmakers, 2016) to assess statistical significance of the correlation between NAR and two-flash fusion threshold. The use of the Bayesian approach allowed us to stop collecting data, analyse the data and then, based on the results, deciding whether or not to continue collecting more data, with an increasing of type I errors rates much lower than the rate we would obtain by using Null Hypothesis Significance Testing (NHST) (Rouder, 2014; Schönbrodt, 2017).

The Bayesian hypothesis testing is based on the Equation (1), where the left term corresponds to the prior odds, the middle term to the Bayes Factor and the right term to the posterior odds. The prior odds are defined as the relative plausibility of the rival hypotheses before seeing the data, that in our case, were set to 1 since both hypotheses were equally plausible a priori (see below). The posterior odds indicate the relative plausibility of the rival hypotheses after having seen the data, meaning that it is the updated version of your first belief. Thus, the Bayes Factor (BF10) quantifies the amount of evidence provided by the data in favour of one of the two hypothesis (Jeffreys, 1961; Kass et al., 1995). For instance, if the BF10 equals 4, it means that the data is 4 times more likely under the alternative hypothesis than under the null hypothesis. By contrast, when the BF10 equals 0.25, the data are 4 times more likely under the null hypothesis than the alternative hypothesis.

$$\underbrace{\frac{p(H_1)}{p(H_0)}}_{Prior\ odds} \times \underbrace{\frac{p(D|H_1)}{p(D|H_0)}}_{Bayes\ Factor} = \underbrace{\frac{p(H_1|D)}{p(H_0|D)}}_{Posterior\ odds} \qquad (1)$$

Regarding our hypothesis, we stated that there should exist a correlation between the NAR and visual temporal resolution, so that higher NAR positively correlates with finer visual temporal resolution. Since we used the two-flash fusion threshold as a measure for visual temporal resolution, and threshold is inversely proportional to resolution, our hypothesis can be translated into an expected negative correlation between the NAR and the two-flash fusion threshold.

To quantify the evidence provided by the data for the presence or absence of a negative correlation $\rho$ between the NAR and the two-flash fusion threshold, we needed to contrast two statistical models. Therefore, we compared the null hypothesis ($H_0$) to a one-sided alternative hypothesis ($H_-$). The alternative hypothesis held a negative correlation between the NAR and the two-flash fusion threshold ($H_-: \rho < 0$), whereas the null hypothesis held no correlation between the NAR and the two-flash fusion threshold ($H_0: \rho = 0$), where $\rho$ denotes Pearson correlation coefficient. To complete the specification of our statistical model $H_-$, we assigned a uniform prior distribution from -1 to 0, $H_-: \rho \sim U(-1,0)$, since all negative values for $\rho$ were equally likely before seeing the data. Once the data was included in the analysis, the $\rho$ prior distribution was updated providing the $\rho$ posterior distribution and the Bayes Factor was computed (Jeffreys, 1961), which was used for the statistical inference. All the Bayesian analyses were performed in a free and open-source software, JASP (https://jasp-stats.org/; JASP Team, 2020).

The stopping criteria previously defined in the study preregistration was that once we arrived at the minimum of 20 subjects, we would finish data collection if the BF10 was below 0.3 (moderate evidence favouring null hypothesis) or above 3 (moderate evidence favouring alternative hypothesis), according to Jeffreys' (1961) interpretation scale. If the BF10 was between 0.3 and 3, we had to collect another subject and calculate the BF10. This procedure was planned to be iterated until we obtain a BF10 outside the (0.3-3) range, or when data from 50 subjects were acquired.

### 5.2 Inclusion/exclusion criteria

The participants were selected following the inclusion criteria established in the preregistration: they were all healthy adults under no medication, not colour-blind, that could perform the binocular rivalry task without glasses nor contact lenses.

In the analyses, only participants that fulfilled all the following (included in the pre-register form) requirements were included:

- Based on the BR task, subjects must have reported more than 50 percepts and they must have reported no clear percept for less than 50% of the time. This criterion was selected in order to ensure a sufficient number of percepts for the NAR estimation.

- Based on the two-flash fusion task, subjects must have not presented near chance performance at all ISIs. Also, the psychometric function had to converge and its slope had to be positive.

## 6. Results

Participants gave explicit consent to participate in the study in accordance with the Declaration of Helsinki. All participants were naïve, and they were paid 10€/hour for participating in the experiment. The protocol of the experiment was approved by the Institutional Committee for Ethical Review of Projects at Universitat Pompeu Fabra (CIREP-UPF).

Due to a dephasing between the analyses and the number of subjects we contacted we finally collected data from 26 participants. However, we considered only the first 20 to compute the Bayes Factor and since it was below 0.3 we stopped collecting more data, basing our results and discussion only in these 20 subjects as we stated in the preregistration. One single subject was discarded for reporting less than 50 percepts and having no clear percept for more than 50% of the time. Therefore, the analysis included 20 subjects (11 female) from the total collected sample of 25 subjects (16 female). The participants' age ranged between 18 and 34 years old.

### 6.1 Reality checks

As a measure to check that the paradigm worked as we expected and that pooled data did not introduce any difference on the results, the following reality checks have been included.

In the BR paradigm, the isoluminance was correctly adjusted as no significant difference between proportion times reported for red and green percepts was seen (see Appendix B). In addition, at a group level, the normalised percept duration probability density function was shaped as a gamma function, meaning unimodal right skewned distribution (Brascamp et al., 2005).

In the two-flash fusion paradigm, subjects were not biased towards a predilect location of the stimuli since there were no significant difference between the hit rate for left and right stimuli (see Appendix B).

### 6.2 Descriptive analysis

The individual distributions of the percept durations obtained from the Binocular Rivalry task are shown in the Appendix C. The mean NAR of the whole sample was 0.313 Hz with a SD = ±0.095 (Hz). To compute the NAR, we used on average 233±85 percepts per participant. Fig. 7A displays the probability density function of the whole percept duration dataset normalised for each subject's median, which was fitted with a gamma function (Brascamp et al., 2005).

The psychometric curves from the two-flash task obtained for each subject can be observed in Appendix C, where variability between subjects is reflected. From the 26 subjects, 8 subjects showed a deviance of the fit of the original dataset with a $p<0.05$, giving evidence to reject the null hypothesis that our model was correctly capturing the subject's psychometric curve. The sample is characterised by a mean two-flash fusion threshold of 37 ms with a SD = ±6 ms, meaning that on average, our subgroup needed at least an interval of 37 ms between two visual stimuli to correctly distinguish them from one single stimulus, at least 75% of the times. The mean hit rate regardless of the ISI and trial type is 68% with a SD = ±6%. The mean response time regardless of the ISI, trial type and correct response is 0.5 s with a SD = ±0.6 s. The psychometric curve of a representative subject (subj. 10) is plotted in figure Fig. 7B.

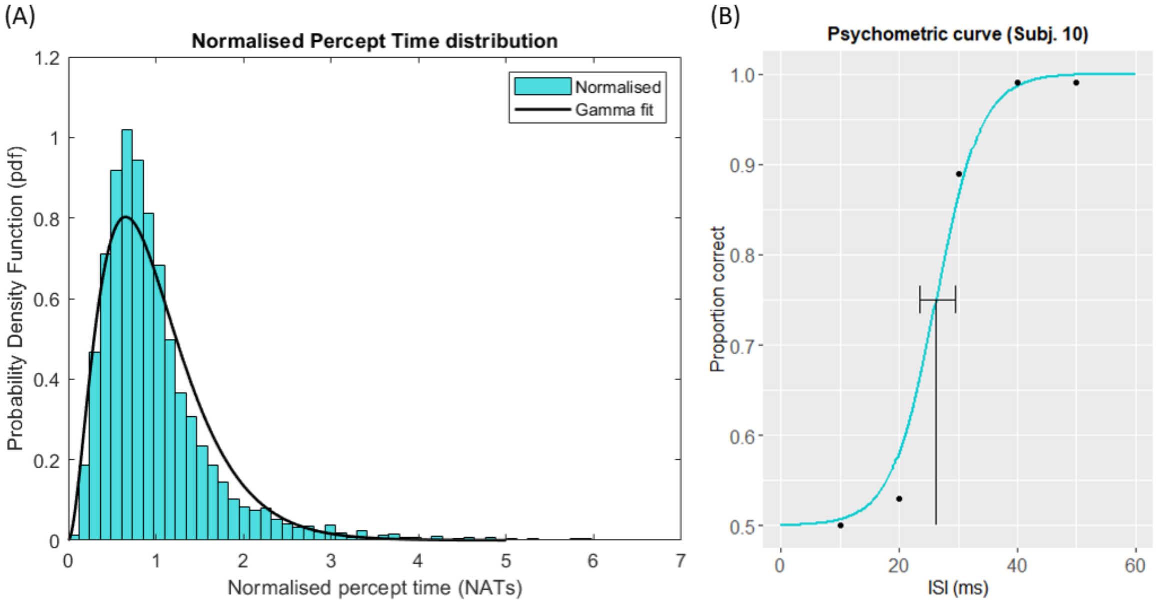

**Figure 7.** Descriptive results for each task. (A) Probability density function (pdf) of the normalised percept durations (Natural Alternation Time units) for the whole dataset, fitted

with a gamma function. (B) Proportion of correct responses regardless of the trial type for each ISI (black dots) fitted with the logistic function (blue line), representing the psychometric curve for subject 10.

### 6.3 Bayesian correlation

With the 20 first subjects collected we plotted the NAR as a function of the two-flash fusion threshold (Fig. 8) resulting in a Pearson's coefficient correlation of $\rho = 0.235$.

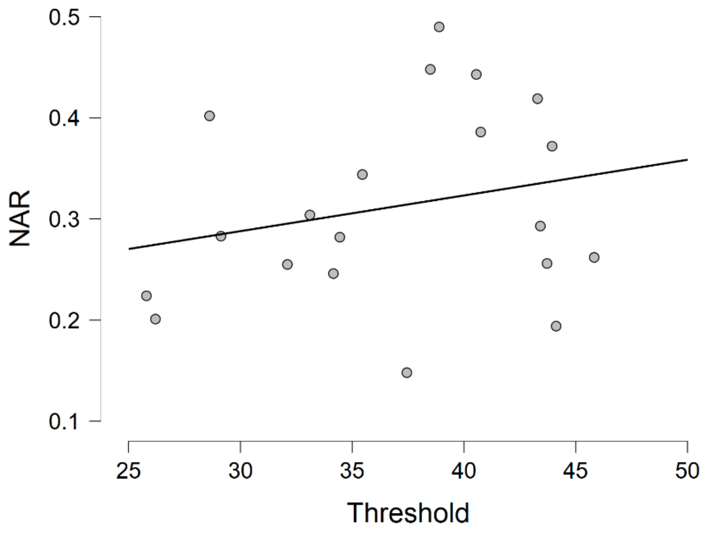

**Figure 8.** Scatterplot of the NAR as a function of the two-flash fusion threshold for the sample size of 20 subjects. The continuous black line corresponds to the trend line. Figure from JASP.

The Bayesian analysis performed with these 20 first subjects resulted in a one tailed Bayes Factor of $BF_{-0} = 0.151 < 0.3$ which implied stopping collecting data. Note that the subscripts "-0" in $BF_{-0}$ indicate that $H_{-}$ is in the numerator of Eq.1 and $H_0$ is in the denominator, meaning that data gave moderate evidence in favour of the null hypothesis. The result is more visible in the prior and posterior distribution plot in Figure 9. Although we hypothesised a negative correlation between the NAR and the two-flash fusion threshold, represented as a uniform prior distribution of $\rho$ within (-1,0), after considering the collected data, the updated distribution of $\rho$ within the same boundaries is skewed to the 0 value (posterior distribution). The interpretation of the posterior distribution plot is that if the $\rho$ value is restricted within -1 and 0, it is most likely to have a near 0 or 0 value, thus, supporting the null hypothesis ($H_0$: $\rho = 0$). Indeed, the ratio of the height of the prior and posterior distribution at $\rho = 0$ (filled dots), equals the evidence that the data provided for $H_-$ versus $H_0$, that corresponds to the $BF_{-0}$ (Wagenmakers et al., 2010). Given that Bayesian analysis allows to quantify the evidence for the null hypothesis (or absence of correlation) (Wagenmakers, 2016), it is more intuitive to express the result in terms of the null hypothesis, that is $BF_{0-}$ corresponding to the inverse of $BF_{-0}$. Therefore, since $BF_{0-} = 6.634$, it means that the data is 6.634 times more likely under the null hypothesis than under the alternative hypothesis, which corresponds to a moderate evidence in the Jeffreys scale (Jeffreys, 1961).

As we performed a sequential analysis using Bayesian statistics, we can see in Figure 10 how the Bayes Factor has been changing as the number of tested subjects increased until it reached the final sample size of n=20. Note that the decreasing tendency was present from the beginning and it seems even to continue decreasing for higher number of subjects before it stabilises.

Since we had collected a larger sample (N=25) we also have included the results of the analysis in the Appendix D as an additional analysis. We obtained the results in line with the previously showed for the n=20 sample: $\rho = 0.237$, $BF_{0-} = 7.985$, giving even stronger evidence in favour of the null hypothesis.

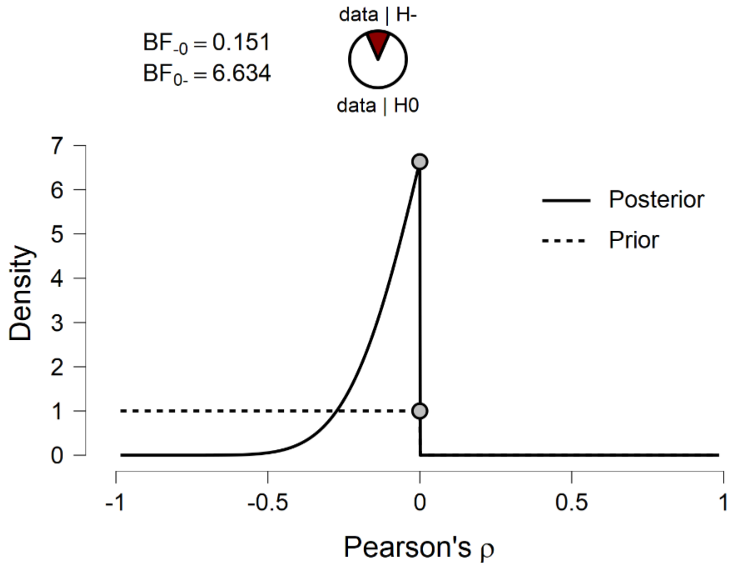

**Figure 9.** Prior and posterior probability density functions for the correlation $\rho$ between the NAR a d the two-flash fusion threshold for the n=20 sample. Both distributions are restricted within the (-1,0) interval. Filled dots correspond to the height of the prior and posterior distributions evaluated at $\rho = 0$. The probability wheel on the top visualises the evidence that the data provide for the two rival hypothesis. Figure from JASP.

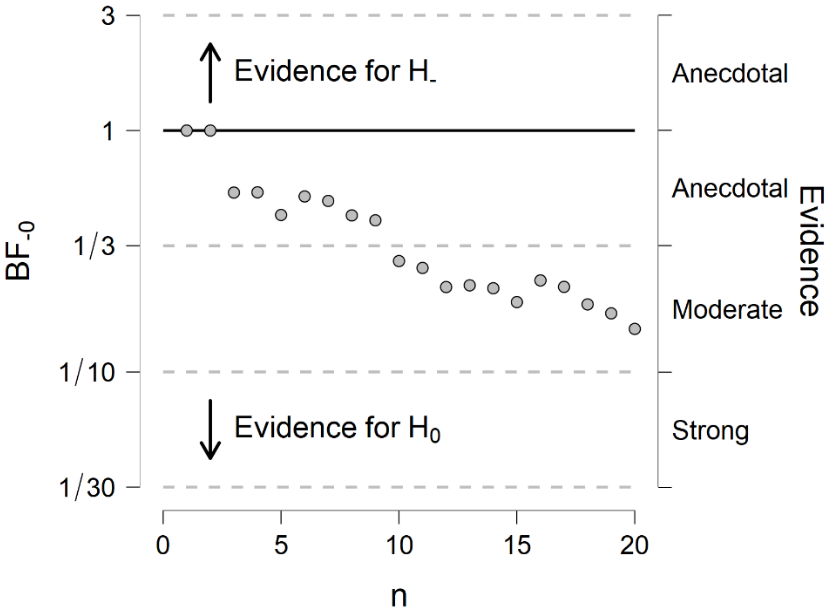

**Figure 10**. The Bayes Factor sequential analysis plot with the heuristic classification of the evidence for each hypothesis. Figure from JASP.

### 6.4 Post-hoc analysis

One could argue, after seeing the plotted data in Fig. 8, that there may exist a correlation in the opposite direction as we hypothesised, meaning a positive correlation between the NAR and the two-flash fusion threshold. Although this potential positive correlation would be difficult to interpret, and it should be taken with caution, given it was evaluated after performing the planned statistical test, we performed a post-hoc two-sided analysis that tested the existence of a correlation between the two variables without considering any prior belief of directionality. Thus, the prior distribution of the $\rho$ for the alternative hypothesis was not restricted within -1 to 0, but it could get any value from -1 to 1, all of them with equal probability ($H_1: \rho \sim U(-1,1)$), as it is reflected in the prior distribution in Figure 11A. The null hypothesis remained the same ($H_0: \rho = 0$).

The results showed a $BF_{10} = 0.44$ -or the equivalent $BF_{01} = 2.27$- that did not give a conclusive evidence in favour of one of the rival hypotheses, although if anything it weakly supported the null hypothesis with anecdotal evidence. The posterior distribution of $\rho$ can be now shaped as a wide normal distribution slightly shifted to positive values of the Pearson's correlation coefficient (Fig. 11A), reflecting thus the inconclusive evidence of the data in favour of one of the hypotheses. The Bayes Factor sequential analysis (Fig. 11B) shows a tendency of evidence for $H_0$ that stabilises with larger n to an anecdotal evidence with $BF_{10} \leq 1/3$, meaning that although we cannot conclude anything from our dataset, we expect the same anecdotal (almost moderate) evidence in favour of the null hypothesis for larger a sample size, in line with the one-sided analysis.

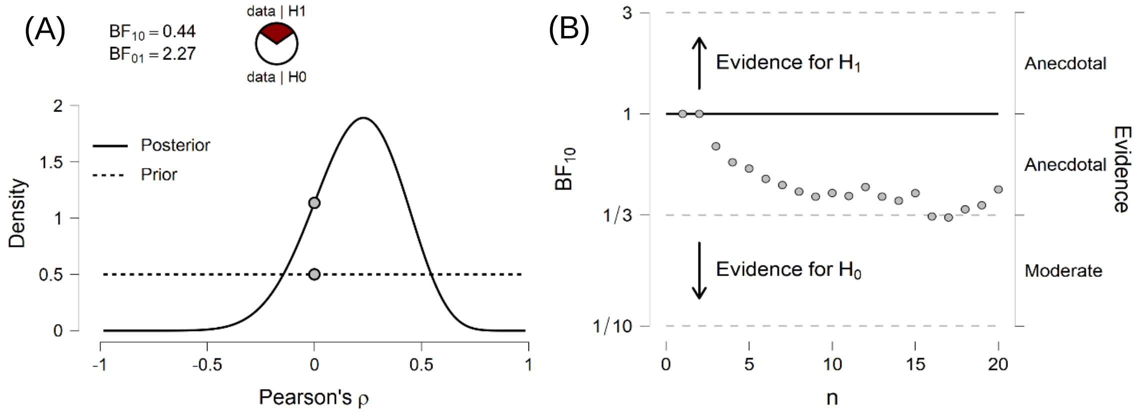

**Figure 11.** Post-hoc analysis results. (A) Prior and posterior probability density functions of $\rho$ for the two-sided test., including the Bayes Factors values as well as the probability wheel. (B) Bayes Factor sequential analysis plot with evidence classification. Figures from JASP.

Indeed, we performed the post-hoc analysis with our N=25 sample and the results also showed anecdotal evidence in favour of the null hypothesis with a $BF_{10} = 0.459$ (or $BF_{01} = 2.177$), giving no conclusive support to neither hypothesis. The expected saturation in the $BF_{10}$ for larger n is also visible in the sequential analysis for N=25. The plots are visible in the Appendix D.

## 7. Discussion

The data collected in both experiments fulfilled our expectations, since we obtained a convergence for the psychometric curves for all the subjects -once we fixed the lapse rate at 0- and percept duration times of the BR task were shaped with a gamma function.

However, the results of the current study do not support the tested hypothesis, which entailed alpha oscillations act as a sampling mechanism for visual information. If the hypothesis is true, and our assumption right, there should be a correlation between the two-flash fusion threshold and the alternation rate in BR, because in both cases visual evidence accumulation would depend on the speed of alpha oscillations at individual level. We did not find the predicted correlation between the NAR in a BR task and the visual temporal resolution in human adults -or the equivalent negative correlation between the NAR and the two-flash fusion threshold. In addition, the post-hoc analysis served to discard the correlation in the opposite direction, concluding that our data did not allow us to state any correlation between the two variables. Since each of our two phenomena (two-flash fusion and BR dynamics) have showed a correlation with individual alpha frequency separately in previous studies: two-flash fusion task (Samaha and Postle, 2015) and binocular rivalry (Katyal, 2019; Torralba et al., 2020); our initial hypothesis, or else some of the assumptions, were incorrect. We provide some tentative explanations that account for our results.

### 7.1 Task-dependent modulation of alpha frequency

Although alpha frequency has been vastly considered as a stable individual trait variable, linking it to differences between subjects in cognitive functionalities (Klimesch et al., 1996; Cecere et al., 2015; Samaha and Postle, 2015), other studies have shown that alpha frequency can be modulated in a task-dependent manner (Samuel et al., 2018). Previous studies reported an increase in alpha frequency with task difficulty (Osaka, 1984; Heagens et al., 2014) while others showed that it depends on the task, meaning that in some tasks alpha frequency increased with task difficulty, but it decreased with other tasks (Earle, 1988). Recently, Wutz, Samaha et al. (2018) found that alpha frequency decreased during and immediately before stimulus processing when task demands temporal integration, but increased when the task demands visual temporal segregation.

This could account for the results we obtained. One could argue that our protocol measured performance on one task that requires temporal segregation and another that induces integration. On the one hand, the two-flash fusion task clearly induces segregation, since it explicitly requires that the subjects segregate two consecutive stimuli in order to perceive them as two flashes. On the other hand, although not explicitly, one could speculate that BR demands temporal integration. Although stimuli were fixed during the 120 s trial, subjects were asked to continuously report the perceived image and they did not know that the stimulus in the screen remained always the same; thus, in order to better perform the task, they might subjectively try to hold on to a percept unless there were enough accumulation in favour of the rival percept. This means, that during BR one might try to integrate evidence in favour of one percept across time disregarding segregated evidences. If this were the case, our results do not necessarily contradict the perceptual cycles hypothesis since we cannot see the negative correlation effect that we hypothesised due to opposed task-frequency modulation. Indeed, while one task increased the alpha frequency, the other task was decreasing it for the same subject, making impossible to obtain a significant correlation of the two tasks performance in either direction due to a counterbalance effect.

Even if we do not make the temporal integration/segregation distinction of the two tasks, they involve very different cognitive processes just for the mere fact to be different tasks. Therefore, it could be possible that in each task the alpha frequency was modulated in a different way and, perhaps it varied differently among subjects, hiding the expected negative correlation.

However, since the limitation of our experiment was that we did not record EEG signal during the experiment, we cannot corroborate this possible explanation of our results based on task-dependent modulation of alpha frequency.

### 7.2 Alpha frequency change between rest and task

In line with the previous tentative explanation, it has been shown that IAF during tasks can differ from IAF at rest (or with closed eyes) (Haegens et al., 2014; Torralba et al., 2020). Taking this into consideration, it could be possible that IAF changed to a different extent and in a different direction for each task, since there were always a 3 to 5 minutes rest between both tasks and the starting order was also randomised across participants. Although Samaha and Postle (2015) found a robust correlation between IAF at rest, as well as IAF at task, and task performance, Katyal et al. (2019) showed only correlation between IAF at task and NAR, but they did not find any correlation with IAF at rest. Furthermore, Torralba et al. (2020) reported both increase and decrease of alpha peak frequency at BR task with respect to IAF at rest. This can lead to different changes of alpha frequency between rest and BR, and between rest and temporal resolution task, that might hide the possible correlation between IAF at task and task performance in both cases.

Again, this is pure speculation since we have not got the EEG data to corroborate the proposed explanation.

### 7.3 The hypothesis is false

The third possibility entails the most drastic explanation of the results. As it was mentioned in the introduction, recent literature reported no alpha phase modulation of visual task performance (Benwell et al., 2017, 2021; Ruzzoli, Torralba et al., 2019). Thereby, the lack of correlation evidenced in the present study could reflect that, in fact, the oscillatory properties of alpha rhythm, as phase and frequency, are not used as a framing mechanism of the visual input.

## 8. Conclusion

This experiment set out to corroborate a prediction of the perceptual cycles hypothesis: That temporal visual resolution and binocular rivalry dynamics would be correlated. We have not found a correlation between alternation rate in a binocular rivalry task and the two-flash fusion threshold in a visual temporal resolution task, as we hypothesised. Moreover, the results from the post-hoc analysis in which we tested the unsigned correlation between the two measures were inconclusive in favour of one of the hypotheses although they slightly support the null hypothesis. We conclude therefore that our study is not an evidence that supports the alpha rhythm function as a sampling mechanism of the visual input into discrete frames -perceptual cycles theory. However, this outcome can not be taken directly as evidence against the theory since other explanations within the framework of the perceptual cycles hypothesis are possible. We have considered some above.

The objective of this study was to address the previously mentioned correlation as an indirect measure of alpha frequency peak, but at the end, not measuring EEG signal has become a limitation of the study since we needed it in order to account for the observed behavioural results. Therefore, a follow up study adding EEG recording to the same experimental set up would provide an explanation of the current results. Indeed, not only would this modified experiment shed a light on our results and serve to test perceptual cycles hypothesis, but it also would address the current question of how IAF is modulated by different tasks as well as task-rest IAF changes.

## 9. References

Alais, D., & Blake, R. (2005). Binocular rivalry and perceptual ambiguity. In *The Oxford handbook of perceptual organization*.

Aurlien, H., Gjerde, I. O., Aarseth, J. H., Eldøen, G., Karlsen, B., Skeidsvoll, H., & Gilhus, N. E. (2004). EEG background activity described by a large computerized database. *Clinical Neurophysiology*, *115*(3), 665-673.

Battaglini, L., Mena, F., Ghiani, A., Casco, C., Melcher, D., & Ronconi, L. (2020). The effect of alpha tACS on the temporal resolution of visual perception. *Frontiers in psychology*, *11*, 1765.

Benwell, C. S., Coldea, A., Harvey, M., & Thut, G. (2021). Low pre-stimulus EEG alpha power amplifies visual awareness but not visual sensitivity. *European Journal of Neuroscience*.

Benwell, C. S., Tagliabue, C. F., Veniero, D., Cecere, R., Savazzi, S., & Thut, G. (2017). Prestimulus EEG power predicts conscious awareness but not objective visual performance. *Eneuro*, *4*(6).

Berger, H. (1929). Über das elektroenkephalogramm des menschen. *Archiv für psychiatrie und nervenkrankheiten*, *87*(1), 527-570.

Blake, R. (2001). A primer on binocular rivalry, including current controversies. *Brain and mind*, *2*(1), 5-38.

Blake, R., Brascamp, J., & Heeger, D. J. (2014). Can binocular rivalry reveal neural correlates of consciousness?. *Philosophical Transactions of the Royal Society B: Biological Sciences*, *369*(1641), 20130211.

Blake, R., & Logothetis, N. K. (2002). Visual competition. *Nature Reviews Neuroscience*, *3*(1), 13-21.

Blake, R., & Wilson, H. (2011). Binocular vision. *Vision research*, *51*(7), 754-770.

Brascamp, J. W., Van Ee, R., Pestman, W. R., & Van Den Berg, A. V. (2005). Distributions of alternation rates in various forms of bistable perception. *Journal of Vision*, *5*(4), 1-1.

Busch, N. A., Dubois, J., & VanRullen, R. (2009). The phase of ongoing EEG oscillations predicts visual perception. *Journal of Neuroscience*, *29*(24), 7869-7876.

Carter, O. L., & Pettigrew, J. D. (2003). A common oscillator for perceptual rivalries?. *Perception*, *32*(3), 295-305.

Cavanagh, P., MacLeod, D. I., & Anstis, S. M. (1987). Equiluminance: spatial and temporal factors and the contribution of blue-sensitive cones. *JOSA A*, *4*(8), 1428-1438.

Cecere, R., Rees, G., & Romei, V. (2015). Individual differences in alpha frequency drive crossmodal illusory perception. *Current Biology*, *25*(2), 231-235.

Cha, O., & Blake, R. (2019). Evidence for neural rhythms embedded within binocular rivalry. *Proceedings of the National Academy of Sciences*, *116*(30), 14811-14812.

Chakravarthi, R., & VanRullen, R. (2012). Conscious updating is a rhythmic process. *Proceedings of the National Academy of Sciences*, *109*(26), 10599-10604.

Chota, S., & VanRullen, R. (2019). Visual entrainment at 10 Hz causes periodic modulation of the flash lag illusion. *Frontiers in neuroscience*, *13*, 232.

Chota, S., Marque, P., & VanRullen, R. (2020). Occipital Alpha-TMS causally modulates Temporal Order Judgements: Evidence for discrete temporal windows in vision. *bioRxiv*.

Crick, F., & Koch, C. (1998). Consciousness and neuroscience. *Cerebral cortex*, *8*(2), 97-107.

Davidson, M. J., Alais, D., van Boxtel, J. J., & Tsuchiya, N. (2018). Attention periodically samples competing stimuli during binocular rivalry. *Elife*, *7*, e40868.

Dugué, L., Marque, P., & VanRullen, R. (2011). The phase of ongoing oscillations mediates the causal relation between brain excitation and visual perception. *Journal of neuroscience*, *31*(33), 11889-11893.

Earle, J. B. (1988). Task difficulty and EEG alpha asymmetry: an amplitude and frequency analysis. *Neuropsychobiology*, *20*(2), 96-112.

Engel, A. K., Fries, P., & Singer, W. (2001). Dynamic predictions: oscillations and synchrony in top–down processing. *Nature Reviews Neuroscience*, *2*(10), 704-716.

Foxe, J. J., & Snyder, A. C. (2011). The role of alpha-band brain oscillations as a sensory suppression mechanism during selective attention. *Frontiers in psychology*, *2*, 154.

Freeman, A. W. (2005). Multistage model for binocular rivalry. *Journal of neurophysiology*, *94*(6), 4412-4420.

Gilbert CD, Sigman M. (2007). Brain states: top-down influences in sensory processing. Neuron 54:677–696.

Grandy, T. H., Werkle-Bergner, M., Chicherio, C., Schmiedek, F., Lövdén, M., & Lindenberger, U. (2013). Peak individual alpha frequency qualifies as a stable neurophysiological trait marker in healthy younger and older adults. *Psychophysiology*, *50*(6), 570-582.

Gulbinaite, R., van Viegen, T., Wieling, M., Cohen, M. X., & VanRullen, R. (2017). Individual alpha peak frequency predicts 10 Hz flicker effects on selective attention. *Journal of Neuroscience*, *37*(42), 10173-10184.

Haegens, S., Cousijn, H., Wallis, G., Harrison, P. J., & Nobre, A. C. (2014). Inter- and intra-individual variability in alpha peak frequency. *Neuroimage*, *92*, 46-55.

Haegens, S., Luther, L., & Jensen, O. (2012). Somatosensory anticipatory alpha activity increases to suppress distracting input. *Journal of cognitive neuroscience*, *24*(3), 677-685.

Haegens, S., Nácher, V., Luna, R., Romo, R., & Jensen, O. (2011). α-Oscillations in the monkey sensorimotor network influence discrimination performance by rhythmical inhibition of neuronal spiking. *Proceedings of the National Academy of Sciences*, *108*(48), 19377-19382.

Halgren, E. (1990). Human evoked potentials. In *Neurophysiological Techniques* (pp. 147-275). Humana Press.

Harris, A. M., Dux, P. E., & Mattingley, J. B. (2018). Detecting unattended stimuli depends on the phase of prestimulus neural oscillations. *Journal of Neuroscience*, *38*(12), 3092-3101.

JASP Team. (2020). JASP (0.14)[Computer software].

Jeffreys, H. (1961). *Theory of probability*, 3rd edn. Oxford, UK: Oxford University Press.

Jensen, O., & Mazaheri, A. (2010). Shaping functional architecture by oscillatory alpha activity: gating by inhibition. *Frontiers in human neuroscience*, *4*, 186.

Kang, M. S. (2009). Size matters: A study of binocular rivalry dynamics. *Journal of vision*, *9*(1), 17-17.

Kass, R.E., & Raftery, A.E. (1995). Bayes factors. *Journal of the American Statistical Association*, *90*, 773–795.

Katyal, S., He, S., He, B., & Engel, S. A. (2019). Frequency of alpha oscillation predicts individual differences in perceptual stability during binocular rivalry. *Human brain mapping*, *40*(8), 2422-2433.

Kleinschmidt, A., Sterzer, P., & Rees, G. (2012). Variability of perceptual multistability: from brain state to individual trait. *Philosophical Transactions of the Royal Society B: Biological Sciences*, *367*(1591), 988-1000.

Klimesch, W. (1999). EEG alpha and theta oscillations reflect cognitive and memory performance: a review and analysis. *Brain research reviews*, *29*(2-3), 169-195.

Klimesch, W. (2012). Alpha-band oscillations, attention, and controlled access to stored information. *Trends in cognitive sciences*, *16*(12), 606-617.

Klimesch, W., Doppelmayr, M., Schimke, H., & Pachinger, T. (1996). Alpha frequency, reaction time, and the speed of processing information. *Journal of clinical neurophysiology*, *13*(6), 511-518.

Klimesch, W., Sauseng, P., & Hanslmayr, S. (2007). EEG alpha oscillations: the inhibition–timing hypothesis. *Brain research reviews*, *53*(1), 63-88.

Koch, S. P., Koendgen, S., Bourayou, R., Steinbrink, J., & Obrig, H. (2008). Individual alpha-frequency correlates with amplitude of visual evoked potential and hemodynamic response. *Neuroimage*, *41*(2), 233-242.

Leopold, D. A., & Logothetis, N. K. (1996). Activity changes in early visual cortex reflect monkeys' percepts during binocular rivalry. *Nature*, *379*(6565), 549-553.

Leopold, D. A., & Logothetis, N. K. (1999). Multistable phenomena: changing views in perception. *Trends in cognitive sciences*, *3*(7), 254-264.

Linares, D., & López-Moliner, J. (2016). quickpsy: An R package to fit psychometric functions for multiple groups. *The R Journal, 2016, vol. 8, num. 1, p. 122-131*.

Luo, C., VanRullen, R., & Alamia, A. (2021). Conscious perception and perceptual echoes: a binocular rivalry study. *Neuroscience of Consciousness*, *2021*(1), niab007.

Mamassian, P., & Goutcher, R. (2005). Temporal dynamics in bistable perception. *Journal of Vision*, *5*(4), 7-7.

Migliorati, D., Zappasodi, F., Perrucci, M. G., Donno, B., Northoff, G., Romei, V., & Costantini, M. (2020). Individual Alpha Frequency Predicts Perceived Visuotactile Simultaneity. *Journal of cognitive neuroscience*, *32*(1), 1-11.

Miller, S. M., Hansell, N. K., Ngo, T. T., Liu, G. B., Pettigrew, J. D., Martin, N. G., & Wright, M. J. (2010). Genetic contribution to individual variation in binocular rivalry rate. *Proceedings of the National Academy of Sciences*, *107*(6), 2664-2668.

Milton, A., & Pleydell-Pearce, C. W. (2016). The phase of pre-stimulus alpha oscillations influences the visual perception of stimulus timing. *Neuroimage*, *133*, 53-61.

Minami, S., & Amano, K. (2017). Illusory jitter perceived at the frequency of alpha oscillations. *Current Biology*, *27*(15), 2344-2351.

Necker, L. A. (1832). LXI. Observations on some remarkable optical phænomena seen in Switzerland; and on an optical phænomenon which occurs on viewing a figure of a crystal or geometrical solid. *The London, Edinburgh, and Dublin Philosophical Magazine and Journal of Science*, *1*(5), 329-337.

Osaka, M. (1984). Peak alpha frequency of EEG during a mental task: Task difficulty and hemispheric differences. *Psychophysiology*, *21*(1), 101-105.

Paffen, C., & Alais, D. (2011). Attentional modulation of binocular rivalry. *Frontiers in Human Neuroscience*, *5*, 105.

Pápai, M. S., Cuello, M. T., Bayer, M., & Soto-Faraco, S. (2018). Occipital Alpha modulates the processing of suppressed visual stimuli during binocular rivalry.

Piantoni, G., Kline, K. A., & Eagleman, D. M. (2010). Beta oscillations correlate with the probability of perceiving rivalrous visual stimuli. *Journal of Vision*, *10*(13), 18-18.

Polonsky, A., Blake, R., Braun, J. & Heeger, D. J. (2000). Neuronal activity in human primary visual cortex correlates with perception during binocular rivalry. *Nature Neurosci.* **3**, 1153–1159.

Prins, N. (2012). The psychometric function: The lapse rate revisited. *Journal of Vision*, *12*(6), 25-25.

Pylyshyn, Z. (1999). Is vision continuous with cognition?: The case for cognitive impenetrability of visual perception. *Behavioral and brain sciences*, *22*(3), 341-365.

Rees, G., Kreiman, G., & Koch, C. (2002). Neural correlates of consciousness in humans. *Nature Reviews Neuroscience*, *3*(4), 261-270.

Ronconi, L., Busch, N. A., & Melcher, D. (2018). Alpha-band sensory entrainment alters the duration of temporal windows in visual perception. *Scientific reports*, *8*(1), 1-10.

Rouder, J.N. Optional stopping: No problem for Bayesians. *Psychon Bull Rev* **21,** 301–308 (2014).

Ruzzoli, M., Torralba, M., Fernández, L. M., & Soto-Faraco, S. (2019). The relevance of alpha phase in human perception. *Cortex*, *120*, 249-268.

Samaha, J., Iemi, L., & Postle, B. R. (2017). Prestimulus alpha-band power biases visual discrimination confidence, but not accuracy. *Consciousness and cognition*, *54*, 47-55.

Samaha, J., LaRocque, J. J., & Postle, B. R. (2020). Spontaneous alpha-band amplitude predicts subjective visibility but not discrimination accuracy during high-level perception. *bioRxiv*.

Samaha, J., & Postle, B. R. (2015). The speed of alpha-band oscillations predicts the temporal resolution of visual perception. *Current Biology*, *25*(22), 2985-2990.

Samuel, I. B. H., Wang, C., Hu, Z., & Ding, M. (2018). The frequency of alpha oscillations: task-dependent modulation and its functional significance. *Neuroimage*, *183*, 897-906.

Schönbrodt, F. D., Wagenmakers, E. J., Zehetleitner, M., & Perugini, M. (2017). Sequential hypothesis testing with Bayes factors: Efficiently testing mean differences. *Psychological methods*, *22*(2), 322.

Team, R. C. (2013). R: A language and environment for statistical computing.

Torralba, M., Drew, A., San José, A. S., Fernández, L. M., & Soto-Faraco, S. (2020). Alpha fluctuations regulate the accrual of visual information to awareness. *bioRxiv*.

Thut, G., Nietzel, A., Brandt, S. A., & Pascual-Leone, A. (2006). α-Band electroencephalographic activity over occipital cortex indexes visuospatial attention bias and predicts visual target detection. *Journal of Neuroscience*, *26*(37), 9494-9502.

Tong, F. (2001). Competing theories of binocular rivalry: A possible resolution. *Brain and Mind*, *2*(1), 55-83.

Tong, F., Meng, M., & Blake, R. (2006). Neural bases of binocular rivalry. *Trends in cognitive sciences*, *10*(11), 502-511.

Tong, F., Nakayama, K., Vaughan, J. T., & Kanwisher, N. (1998). Binocular rivalry and visual awareness in human extrastriate cortex. *Neuron*, *21*(4), 753-759.

Ukai, K., Ando, H., & Kuze, J. (2003). Binocular rivalry alternation rate declines with age. *Perceptual and motor skills*, *97*(2), 393-397.

Valera, F. J., Toro, A., John, E. R., & Schwartz, E. L. (1981). Perceptual framing and cortical alpha rhythm. *Neuropsychologia*, *19*(5), 675-686.

VanRullen, R. (2016). Perceptual cycles. *Trends in cognitive sciences*, *20*(10), 723-735.

VanRullen, R., & Koch, C. (2003). Is perception discrete or continuous?. *Trends in cognitive sciences*, *7*(5), 207-213.

Von Stein, A., Chiang, C., & König, P. (2000). Top-down processing mediated by interareal synchronization. *Proceedings of the National Academy of Sciences*, *97*(26), 14748-14753.

Wagenmakers, E. J., Lodewyckx, T., Kuriyal, H., & Grasman, R. (2010). Bayesian hypothesis testing for psychologists: A tutorial on the Savage–Dickey method. *Cognitive psychology*, *60*(3), 158-189.

Wagenmakers, E. J., Verhagen, J., & Ly, A. (2016). How to quantify the evidence for the absence of a correlation. *Behavior research methods*, *48*(2), 413-426.

Wichmann, F. A., & Hill, N. J. (2001). The psychometric function: I. Fitting, sampling, and goodness of fit. *Perception & psychophysics*, *63*(8), 1293-1313.

Wilson, H. R. (2003). Computational evidence for a rivalry hierarchy in vision. *Proceedings of the National Academy of Sciences*, *100*(24), 14499-14503.

Wutz, A., Melcher, D., & Samaha, J. (2018). Frequency modulation of neural oscillations according to visual task demands. *Proceedings of the National Academy of Sciences*, *115*(6), 1346-1351.

Zhang, P., Jamison, K., Engel, S., He, B., & He, S. (2011). Binocular rivalry requires visual attention. *Neuron*, *71*(2), 362-369.

## 10. Statement of contribution

My contribution to the study consisted of:

- Temporal calibration of the stimuli in the two-flash fusion task.
- Pilot data collection and analysis.
- Contributing to experimental design.
- Programming the two-flash fusion experiment.
- Preregistering form.
- Data collection of the 26 participants.
- Performing Binocular Rivalry data analysis.
- Programming and performing two-flash fusion data analysis.
- Bayesian statistical analysis.
- Figures and visualisation preparation
- Results interpretation
- Writing the manuscript

# 11. Appendices

## Appendix A

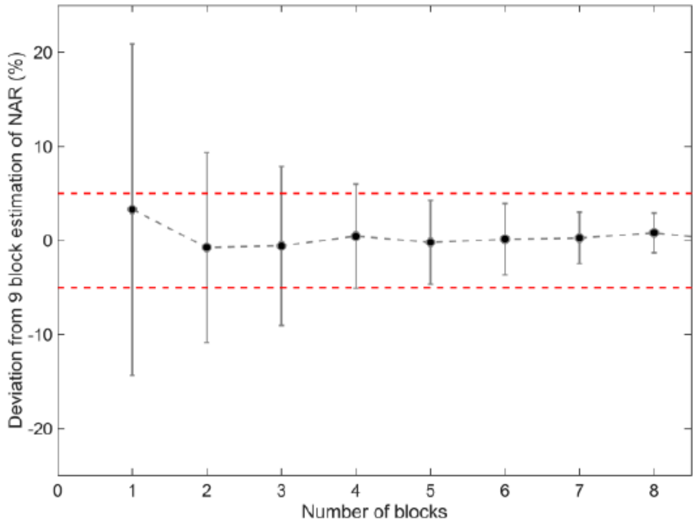

**Figure A1.** Deviation of NAR for 9 block estimation of NAR as a function of the number of blocks, from Torralba et al., (2020) experiment.

## Appendix B

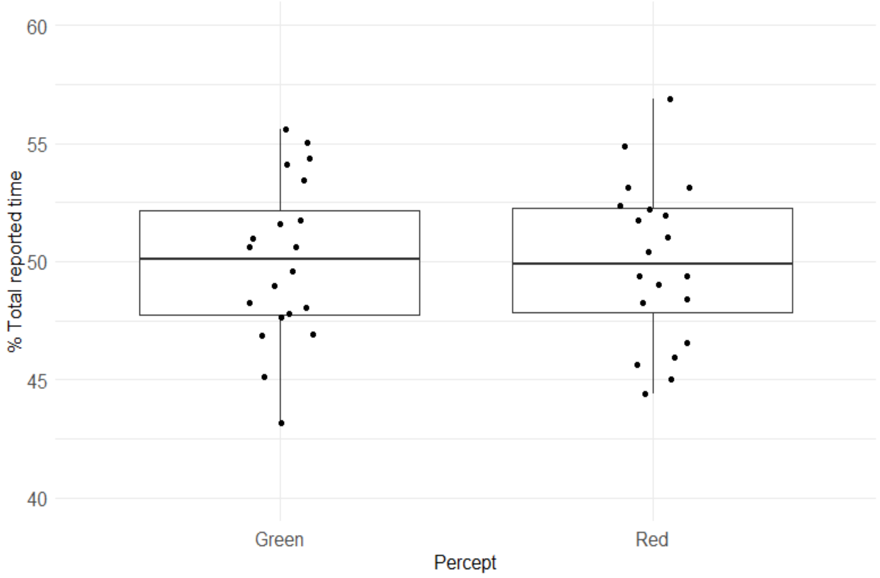

**Figure B1.** Boxplot of the percentage of total dominant percept reported time for each dominant percept (Green and Red). There is no significant difference between them (mean difference = 0.06, SD = ±0.04; p=0.98). Data from the n=20 studied sample.

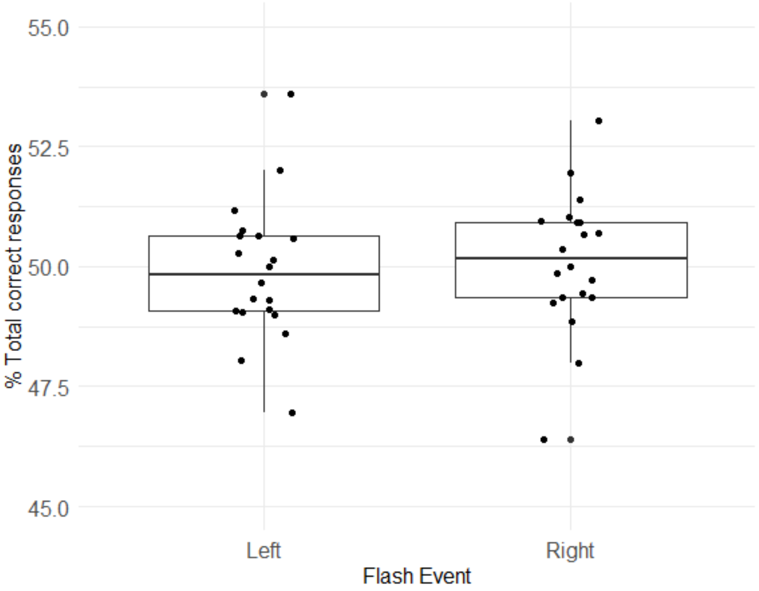

**Figure B2.** Boxplot of the percentage of total correct responses for left and right flash event type, regardless of the ISI. There is no significant difference between them (mean difference = 0.022, SD=± 0.019; p=0.75). Data from the n=20 studied sample.

## Appendix C

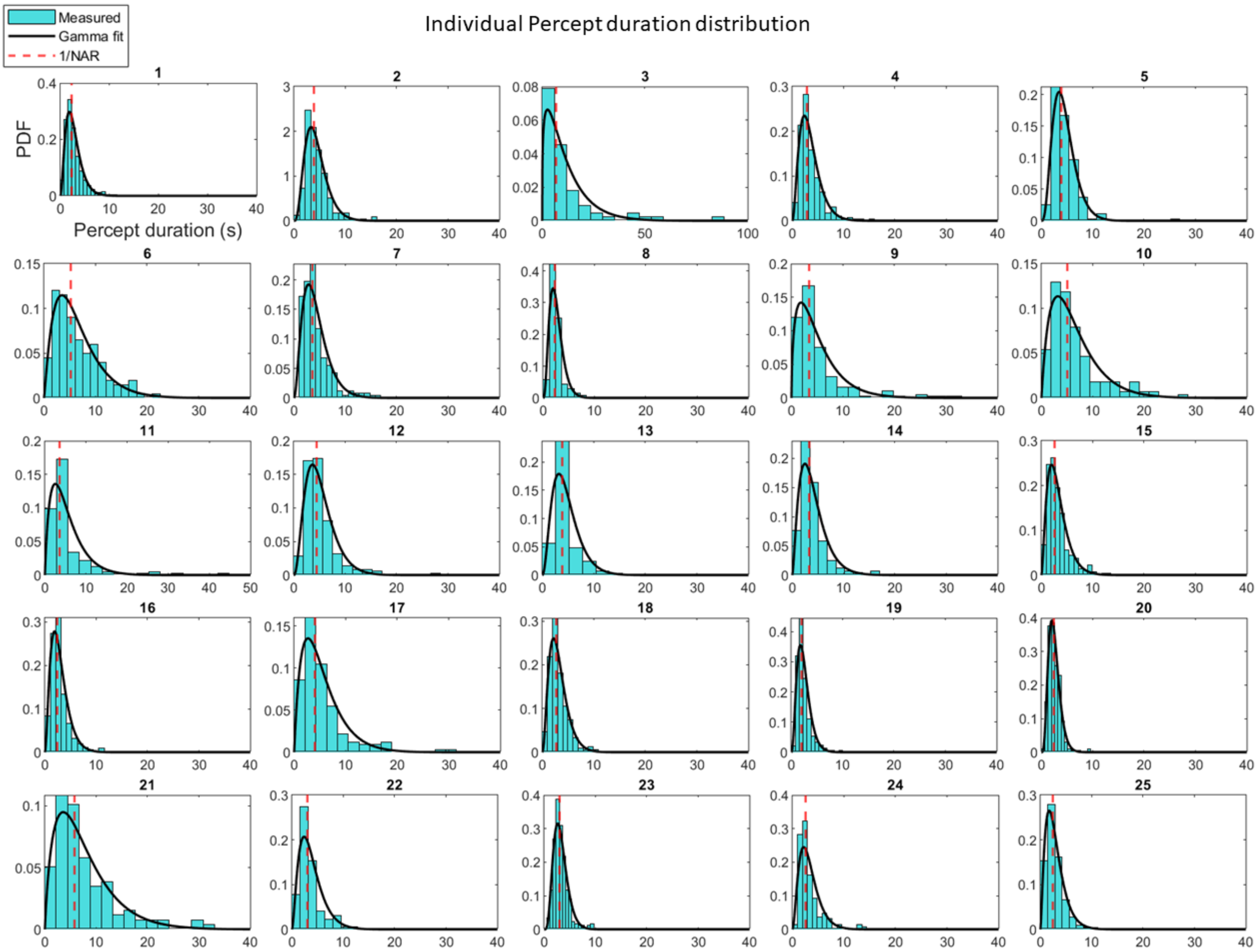

**Figure C1.** Individual plots of the probability density function (PDF) of the percept duration (s). The distributions are fitted with a gamma function and red dashed line indicate the median, corresponding to the inverse of the NAR. Note that plots 3 and 11 have different x axis limits due to longer percepts reported.

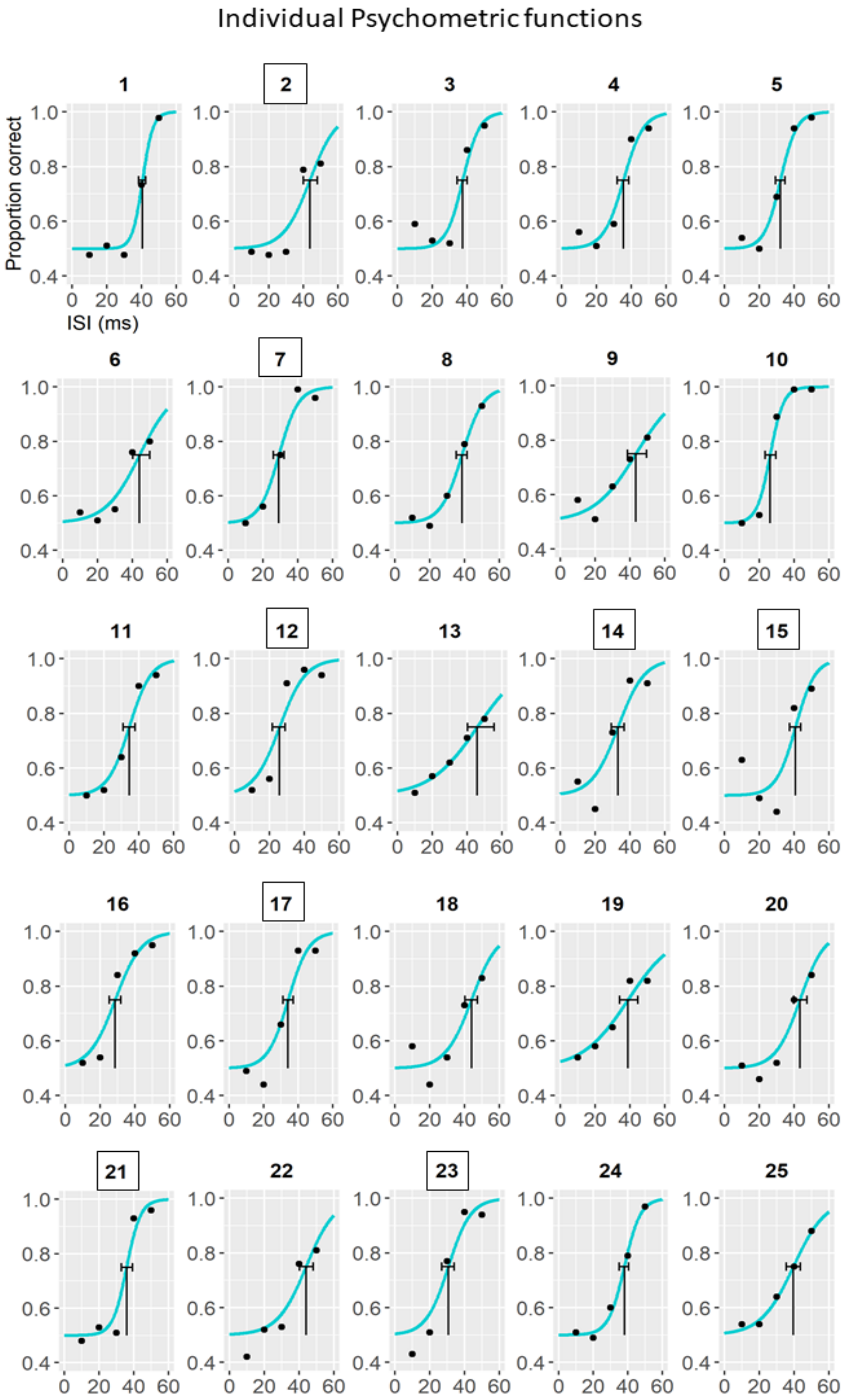

**Figure C2.** Individual plots of the psychometric curve -proportion correct as a function of the inter stimulus interval (ms). Black dots correspond to the actual data while blue curve is the best fit with a logistic function. Two-flash fusion threshold corresponds to the value of the psychometric curve at y=0.75 (indicated with a vertical line), 95% CI is also visible. Black square over the plots indicates fits whose deviance p-value is $p<0.05$.

## Appendix D

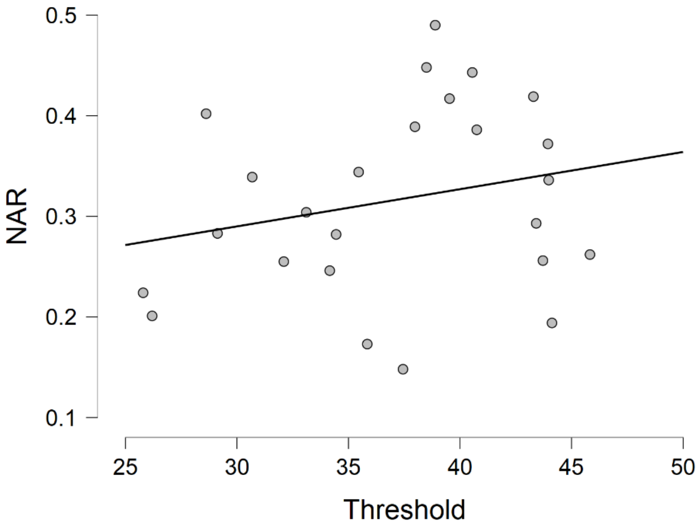

**Figure D1.** Scatterplot of the NAR as a function of the two-flash fusion threshold for the sample size of 25 subjects. The continuous black line corresponds to the trend line. Figure from JASP.

**Bayesian statistics for N=25 (one-sided test)**

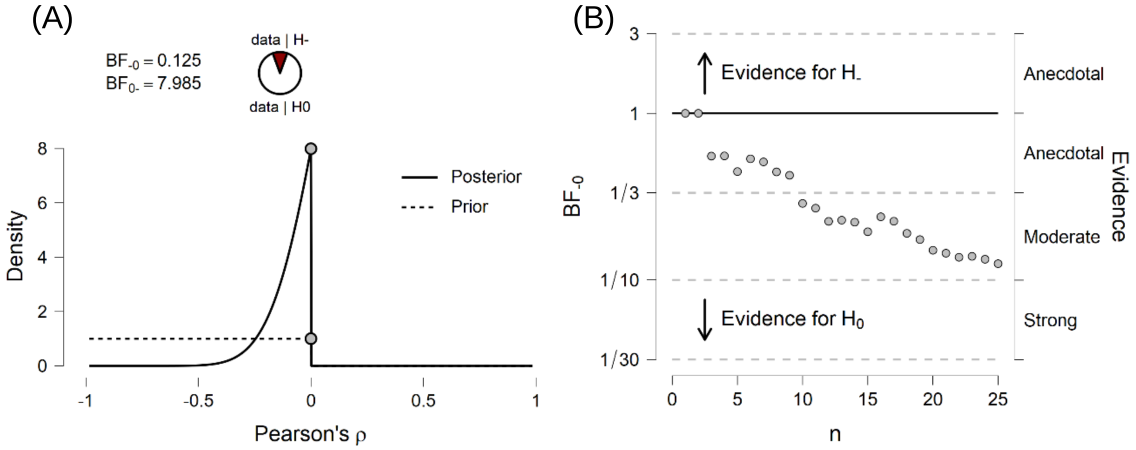

**Figure D2.** Results of the one-sided analysis for the N=25 sample. (A) Prior and posterior probability density functions for $\rho$, including Bayes factor values and probability wheel. (B) Sequential analysis plot. Figures from JASP.

## Bayesian statistics for N=25 (post-hoc analysis)

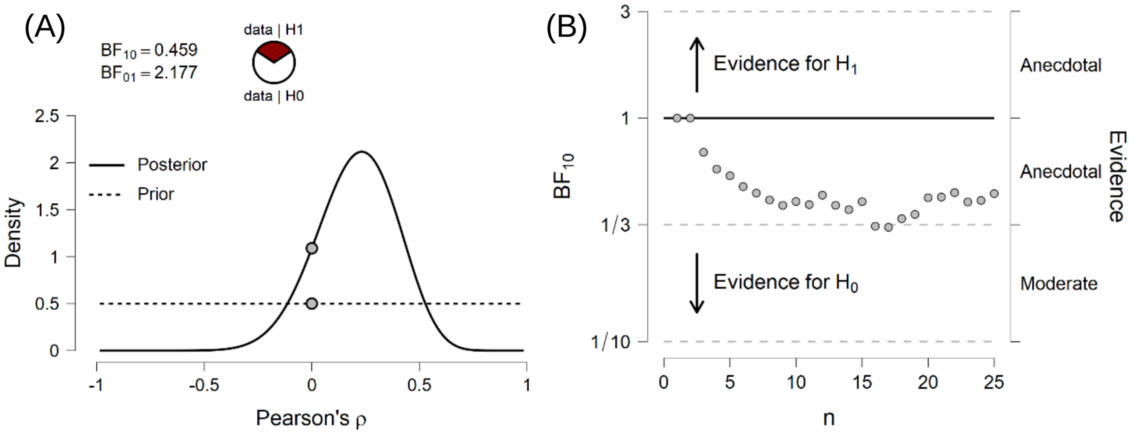

**Figure D3.** Results of the post-hoc analysis for the N=25 sample. (A) Prior and posterior probability density functions for $\rho$, including Bayes factor values and probability wheel. (B) Sequential analysis plot reflecting the saturation of the BF. Figures from JASP.